



Exertion of Modified Mineral and Plant-based Powders in the Sorption of Pb(II) Ions

INDHUMATHY P¹ and MUTHULAKSHMI ANDAL N^{2*}

^{1,2*}Department of Chemistry, PSGR Krishnammal College for Women, Peelamedu,
Coimbatore, Tamil Nadu, India.

*Corresponding author E-mail: muthulakshmiandal@psgrkcw.ac.in

<http://dx.doi.org/10.13005/ojc/400234>

(Received: January 23, 2024; Accepted: March 20, 2024)

ABSTRACT

Heavy metal rich industrial discharges solemnly threaten the condition of ecosystem and human haleness. Lead pollution as a result of various anthropogenic activities is a major concern due to its high toxic nature. Chelating capacities of treated *Magnolia champaca* Barks (TMCB) and treated Attapulgitte Clay Powder (TACP) are investigated in the process of sequestration under lab scale conditions. The sorbent matrices are subjected to microscopic, SEM/EDAX and FTIR analyses to study the variations in the adsorbents surfaces, alterations in the surface morphological characteristics, specific involvement of metal ions and functional group peaks, with respect to the sorption process. Dimensions and masses of sorbents, metal ion concentration, agitating periods, pH and temperature of the analyzed systems are optimized under Batch Equilibration studies. The experimentally verified samples are analyzed using Atomic Absorption Spectrophotometer to determine the Pb(II) ions concentrations. The derived Freundlich and Langmuir isothermal plots based on the experimental results obtained for TMCB–Pb(II)/TACP–Pb(II) exhibited a better linearity for Freundlich model, thereby, supporting multilayer sorption. A judicious comparison made between TACP and TMCB reveals a marginal sorption performance by the former.

Keywords: Heavy metals, Sorption, Sorbents, Sequestration, Isotherm.

INTRODUCTION

Environmental pollution remains the world's most serious problem and is considered as one of the leading causes for sickness and mortality. It is not only triggered by industrialization, exploration, urbanization, population growth, but also by trans boundary movement of pollutants from one region to the other^{1,2}. Degradation of water ecosystem is reasoned, mainly by agricultural runoffs, industrial/municipal let-outs which comprises of various

organic/inorganic pollutants. Amidst various toxicants, heavy metals with specific gravity $> 5 \text{ g/cm}^3$ are non-biodegradable, persistent and hazardous. These toxicants enter the food chain through bioaccumulation and induce damage even in trace concentrations^{3,4,5}.

Lead is the second most toxic metal, accounting for 0.002% of the Earth's crust. It is naturally found in a very limited amount, but enters the environs, due to anthropogenic activities



and contributions from industries manufacturing automobile parts and batteries. Further common sources of exposure include paint contamination (toys, containers, jewellery, etc.), food packaging, and water pipes^{6,7}. In humans, acute lead poisoning produces significant dysfunction in the kidneys, reproductive systems, liver, brain, and central nervous system. Thenceforth, the removal of this noxious element from the water bodies is vital, which has provoked the need for various treatment methodologies^{8,9}.

Several treatment approaches for removal of toxic substances have been documented. Biological substrates, membrane filtration, reverse osmosis, oxidation, electrochemical oxidation, coagulation/flocculation, chemical precipitation, and adsorption lay the foundations for these technologies^{10,11}. Factors such as cost, efficiency, dependability, feasibility, environmental impact, practicability and operational challenges influence the utilization of the aforesaid methods^{12,13,14}.

Adsorption technique stands out due to its flexibility in operation and design procedures and in addition appears to have a considerable impact on the toxicity, biological availability, and transit of heavy metals in wastewater^{15,16,17,18}. Adsorbents used, such as biomass materials, charcoal, sludge ash, microbes, clays and so on, have a large number of active binding sites on their surface via which heavy metals can be successfully retained under certain conditions^{19,20,21}. Thus the background of the present study involves in assessing the effectiveness of a

biomaterial and a clay mineral in the trapping lead ions from aqueous media through batch mode and deriving out of its isothermal fit for the systems.

MATERIALS AND METHODS

Collection and preparation of adsorbents

Two eco-friendly materials (tree bark and mineral) have been identified for the present study. *Magnolia champaca* tree barks collected from the locales of Coimbatore, were washed with double distilled water to remove the scums and then dried thoroughly. The dried barks were crushed and pulverized using an electrical mixer. The second raw material, Attapulgitte a fine clay powder, was purchased from Raisha Enterprise, Gujarat, India. It is composed of magnesium aluminium phyllosilicate (chemical formula- $(\text{Mg,Al})_2\text{Si}_4\text{O}_{10}(\text{OH})\cdot 4(\text{H}_2\text{O})$). Both the native materials were categorized into different mesh sizes using Scientific Test Molecular Sieves.

Modification of the sorbent material

The categorized *Magnolia champaca* Barks (MCB) and Attapulgitte Clay Powder (ACP) were treated with 0.1 N HCl to modify their surface nature. The modified materials are referred to as Treated *Magnolia champaca* Barks (TMCB) and Treated Attapulgitte Clay Powder (TACP). The treated materials were washed several times using doubly distilled water to maintain neutral pH. The chemically modified sorbents were employed for the laboratory experiments. Figs. 1 and 2 (a–c) represent the cleaned materials, sieved powders and their treated counterparts.



Fig. 1(a). MCB



Fig. 1(b). Raw MCB



Fig. 1(c). TMCB



Fig. 2(a). ACP



Fig. 2(b). Raw ACP



Fig. 2(c). TACP

Microscopic Analysis

Pulverized TMCB and TACP were analysed using Optical Microscope (Magnus Microscope CH20ILED) to assess their particle sizes. Mesh size (85BSS, 72BSS, 52BSS, 36BSS and 22BSS) correspond to 0.18 mm, 0.21 mm, 0.30 mm, 0.42 mm and 0.71 mm particle sizes respectively. Microscopic images of native / treated MCB and ACP (0.18 mm) are depicted in Fig. 3 (a,b) and Figure 4 (a,b).

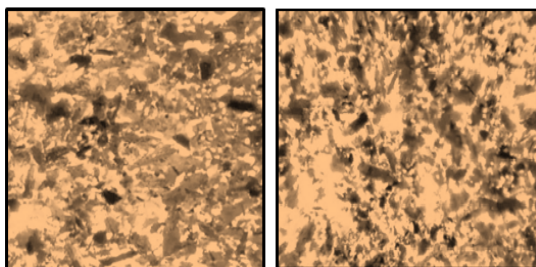


Fig. 3(a). MCB

Fig. 3(b). TMCB

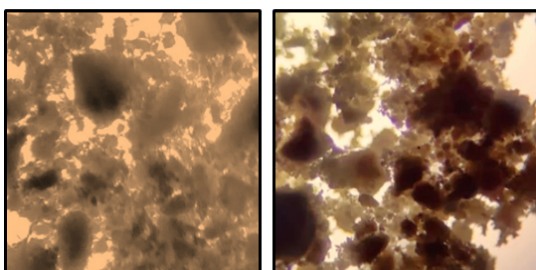


Fig. 4(a). ACP

Fig. 4(b). TACP

Adsorbate (stock solution preparation)

A stock solution of 1000 mg/L was prepared by dissolving 1.5985 g lead nitrate (analytical grade) in doubly distilled water. A standard solution (100 mg/L) was obtained by diluting the stock solution. Further, working aliquots were prepared as appropriate dilutions of the standard solution.

Batch Optimization Studies

Experimental setup in batch mode was planned in such a way that the fixation of varied influential factors are ensured. The operating parameters were contact time period, size and amounts of the sorbent materials, required concentration of the sorbate ions, pH and temperature conditions, presence of cations and anions, to study the sorption efficiencies of TMCB and TACP. 50 mL Pb(II) solutions of desired concentrations (5 to 20 mg/L–5 mg/L interval) were transferred into 250 mL agitation flasks and the varied sorbent doses (TMCB–50 to 250 mg–50 mg interval / TACP–50 to 200 mg–50 mg interval) were added to the solutions. The contents of the flasks were stirred (140 rpm) in

a mechanical shaker under the preset conditions (3 to 30 mins–3 mins interval). The concentrations of Pb(II) ions were determined using Atomic Absorption Spectrophotometer (Shimadzu (AA 6200) model). Pb(II) removal from the aqueous solutions, both at pre and post experimental setup were calculated (%) as follows:

$$\% \text{Removal} = (C_i - C_e) / C_i \times 100$$

Characterization Studies

Involvement of functional groups present in TMCB and TACP sorbents were studied using Shimadzu Fourier Transformation Infra-red Spectrophotometer (4500-500 cm^{-1} range). Peak variations pertaining to these groups were recorded. Assessment of the deviations in surface morphology and elemental constitutions of the processed metal loaded matrices were done using Scanning Electron Microscope (SEM) and Energy Dispersive X-ray Analysis (EDAX) (TESCAN-MIRA3 XMU). The results of these assays are discoursed further.

RESULTS AND DISCUSSION

Fourier-Transform Infrared Spectroscopic Analysis

Fourier-transform infrared spectroscopy (FTIR) is declared as an effectual analytical method to study the vibrational modes of molecules in a sample. Fig. 5(a) and 5(b) correspond to the FTIR spectra of the studied sorbents. The involvement of groups during metal adsorption is inferred from the disappearing peaks in the metal-laden TMCB spectrum with reference to hydroxyl groups (3251 cm^{-1}) and alkoxy groups (1090 cm^{-1}). Narrow peak of C=O stretching at 1629 cm^{-1} recorded a change in its counterpart spectra. Appearance of additional peaks at 2342 cm^{-1} and 2963 cm^{-1} in the post-run spectra suggests the stretching of C-H bonds in the precursor sample. Peaks with noticeable shifts less than 900 cm^{-1} signify variations in C-H bending vibrations which shall be due to the binding property of the metal ion.

An decrease in the intensity of the broad band at 3562 cm^{-1} corresponding to the O-H stretching vibrations is envisaged in the metal laden spectra (Fig. 5(b)) indicating its participation during metal binding on the surface of the sample. Further, the disappearance of peaks (1651 cm^{-1} and

1020 cm^{-1}) characteristic of water molecules present in the silica matrix suffices its metal quenching property. Similar observations were recorded by Song Jingyan *et al.*,²². Appearance of new peaks at 2972 cm^{-1} and 1921 cm^{-1} relating to C–H group and shift of peaks to wave numbers 1166 cm^{-1} and 736 cm^{-1} imply their involvement in the sorption process.

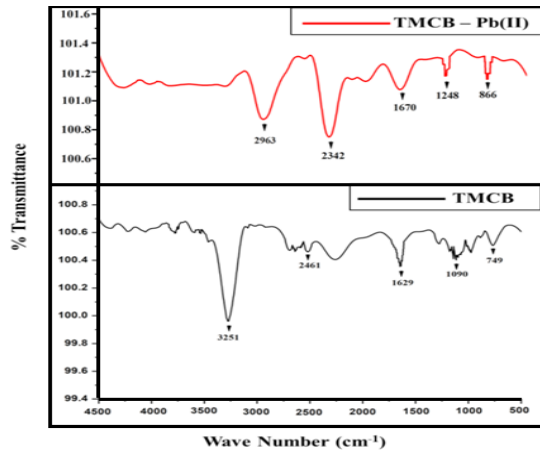


Fig. 5(a). FTIR Spectra–TMCB and TMCB-Pb(II)

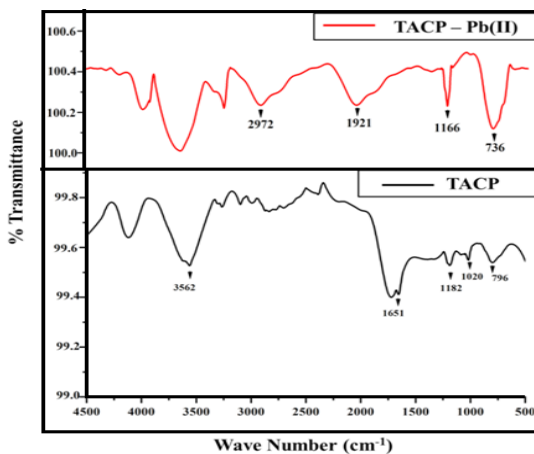


Fig. 5(b). FTIR Spectra–TACP and TACP-Pb(II)

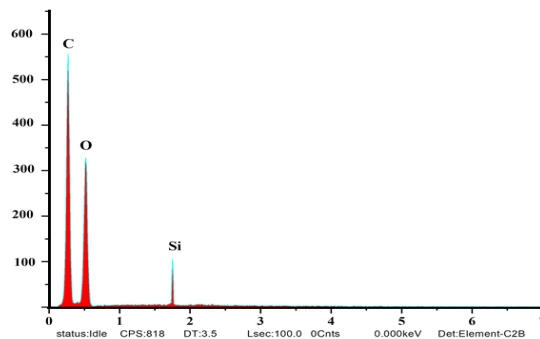


Fig. 8(a). TMCB

Scanning Electron Microscopic Analysis

Scanning Electron Microscopic (SEM) analysis assists high resolution imaging and overtures imperative information on the size, shape and surface structure of the studied materials. Native and metal laden TMCB and TACP materials were subjected to analysis and their corresponding micrographs are pictured in Figs. 6 (a and b) and 7 (a and b). Disappearance of pores and coarse from native samples evidence the covering of pores by Pb(II) ions.

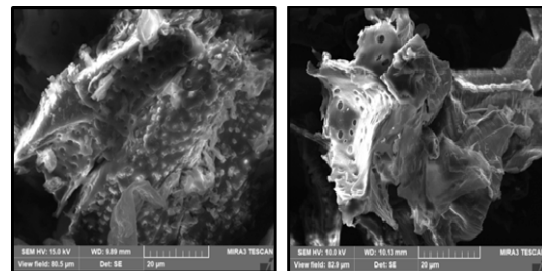


Fig. 6(a). TMCB

Fig. 6(b). TMCB-Pb(II)

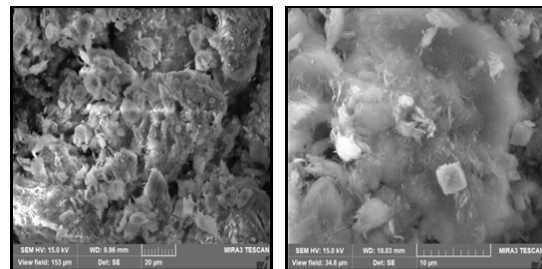


Fig. 7(a). TACP

Fig. 7(b). TACP-Pb(II)

EDAX Analysis

The elemental compositions of the studied sorbents were dogged using Energy-Dispersive X-ray Spectroscopy. Quantitative and qualitative data regarding the specified elements were derived for the samples from the obtained spectra. Pronouncement of new peaks around 2 keV [Figs. 8 (a and b) and 9 (a and b)] confirm the adherence of Pb(II) ions onto the surfaces of TMCB and TACP.

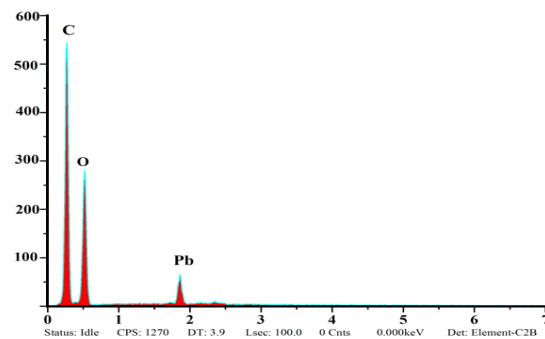


Fig. 8(b). TMCB-Pb(II)

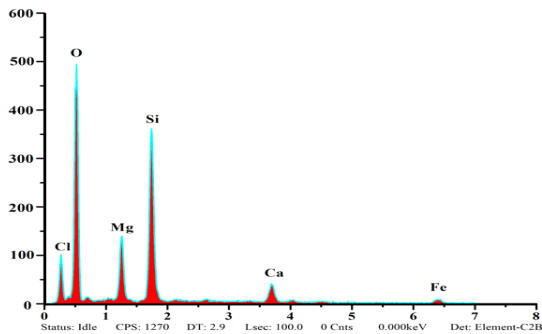


Fig. 9(a). TACP

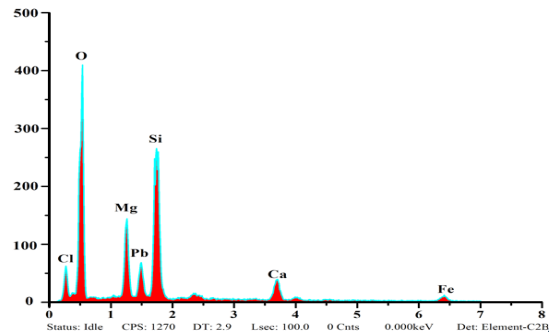


Fig. 9(b). TACP-Pb(II)

Batch Equilibration Studies
Impact of Particle Size

Adsorption kinetics varies significantly under the influence of particle size of samples. Smaller particles possess greater surface area per unit mass compared to larger particles. This in turn enhances the number of adsorption sites, thereby greater adsorption capacity of the former. A plot of percentage removal vs particle size comprising the two systems viz., TMCB–Pb(II)/TACP–Pb(II) is shown in Fig. 10. As per the made statement, Pb(II) ion had been better sorbed by least particle size, i.e. 0.18 mm, further decline, as obvious from the curve. The decrease in percentage removal can also be attributed to the resistance in mass transport property. 0.18 mm particle size was fixed for further experiments.

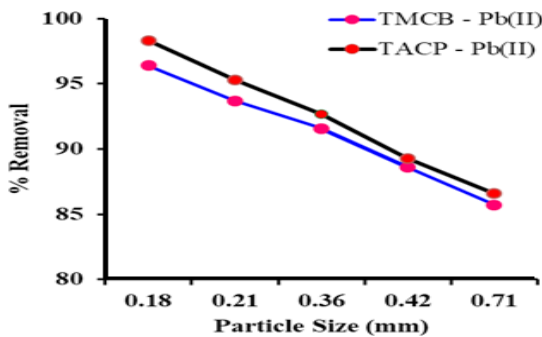


Fig. 10. Impact of Particle Size

Impact of Initial Concentration and Contact Time

Initial ion concentration and contact time are critical parameters in determining a system's sorption efficiency. The sorbing ability of TMCB/TACP at varying initial concentrations (5–20 mg/L; 5 mg/L interval) at distributed time frames (3 to 30 mins; 3 mins interval) is displayed in Fig. 11 (a) and (b) respectively. Rapid sorption occurred at the initial stage shall be due to availability of extended active sites. However, a steep decrease is observed beyond the maximum Pb(II) sorption (96% by TMCB

at 15 mins and 98% by TACP at 9 mins) exhibited by 20 mg/L initial sorbate concentration.

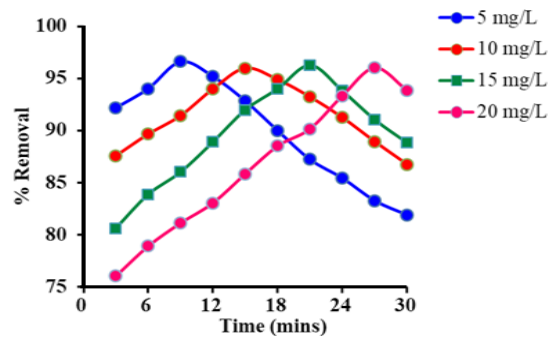


Fig. 11(a). Impact of Initial Concentration and Agitation time–TMCB–Pb(II) system

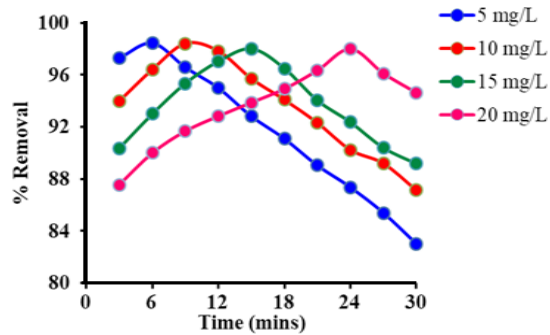


Fig. 11(b). Impact of Initial Concentration and Agitation time–TACP–Pb(II) system

Impact of Dosage

Sorbent dosage is a crucial parameter and must be optimized so as to achieve an efficient metal removal. Batch studies carried out at specific sorbent dosages are depicted in Fig. 12(a) and 12(b). A gradual increase in the peaks corresponding to the removal of Pb(II) ions in TMCB and TACP systems are observed, linearly with the sorbent dose of 200 mg and 150 mg, respectively. Further, downgrading in the removal suggest the saturation of active sites.

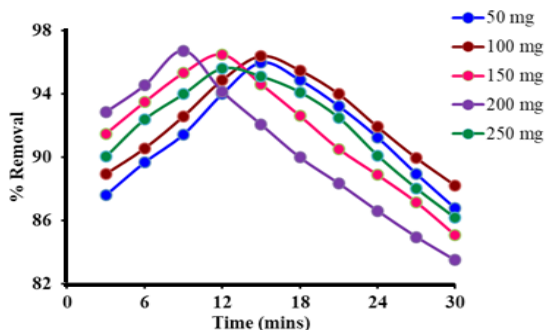


Fig. 12(a). Impact of Dosage–TMCB–Pb(II) system

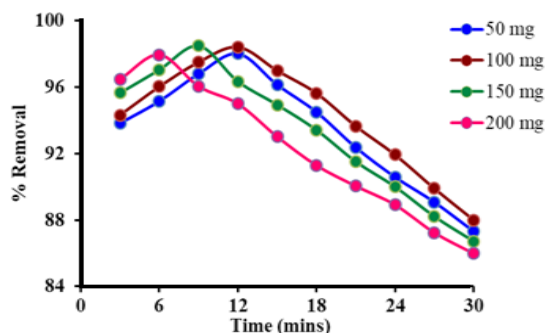


Fig. 12(b). Impact of Dosage–TACP–Pb(II) system

Impact of pH

pH of a solution influences the surface charge of and the adsorbate species which, in turn, impose a substantial effect on the sorption behaviour of any studied system. Experimental observations for pH effect are indicated by the inverted parabolic curves in Fig. 13. A maximum Pb(II) ions removal had occurred at pH 5 in both the cases. Competent nature of H⁺ ions, ahead of Pb(II) ions under acidic conditions and complex forming nature of Pb(II) ions in alkaline medium shall be the driving force for decreased sorptive nature of the divalent ion.

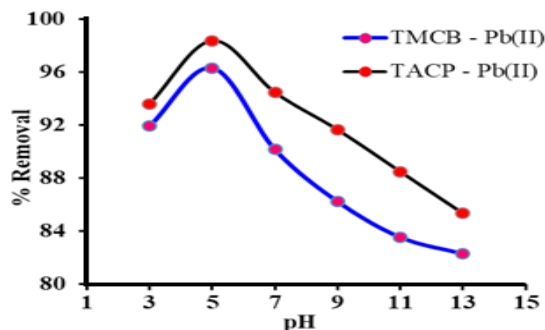


Fig. 13. Impact of pH

Impact of Temperature

Temperature has a significant control over the adsorption capacity, adsorption kinetics and

desorption in the sorption processes, depending on the specific system and application. The sorption of the selected divalent ion was found to increase gradually with rise in temperature from 273 K-313 K for TMCB/273 K-303 K for TACP as indicated by the smooth inclination patterns in Fig. 14. Extending the temperature beyond the respective temperature environs for TMCB–Pb(II)/TACP–Pb(II) systems inhibited sorption, may be due to the denaturing of reaction characteristics as implied by the downfall in the curves.

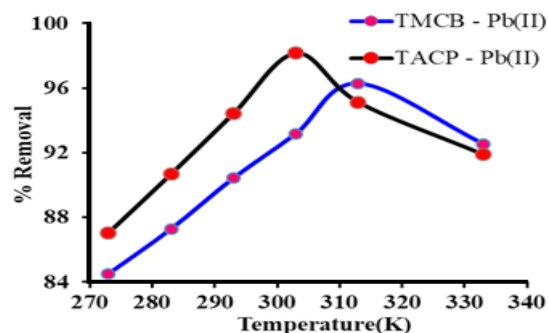


Fig. 14. Impact of Temperature

Impact of Cations/Anions/Co-ions

Unavoidable existence of cations, anions, co-ions ions in natural and industrial water streams, had led to their impeccable study in the process of optimization. Presence of these ions deteriorates the chelating ability of the sorbents as evidenced from the variation of the block heights of the bar chart (Fig. 15). Amongst the studied cations, sorption efficacy was highly subdued due to the presence of K⁺ than Na⁺, the reason can be the small ionic radii of K⁺ and its higher hydration energy. Anionic inhibition is largely extended by Cl⁻ due to the preferential stable chloro complex formation by Pb(II). Pb(II) with larger ionic radii (0.118 nm) than co-metal ions [Zn(II)–(0.074 nm) and Cr(VI)–(0.04 nm)], exhibit appreciable solvation property resulting in a dip in the percentage removal of the former.

Isothermal Studies

Adsorption process is quantified by the adsorption isothermal studies, as they provide deep insights about the interaction between the sorbate and sorbent surfaces. Langmuir and Freundlich isothermal studies were applied to the obtained experimental data for the studied systems [Fig. 16(a) and (b)]. Table 1 lists the Langmuir (q_m , K_L) and Freundlich ($1/n$, K_f) isothermal coefficients derived from the slope and

intercept of the corresponding plots. Tabulated isothermal data show a maximum adsorbing capacity values (q_m) [TMCB-1.89 mg/g; TACP-17.06 mg/g], along with appreciable sorbate-sorbent interaction (K_L) [TMCB-7.19 L/mg; TACP-37.68 L/mg] for the studied systems. The q_m and K_L values is higher for TACP than TMCB, due to its extensive availability of sorption sites and ion exchange capability in the SiO_4 structure of the former. However, better fit has been registered for Freundlich model. This may be due to preferential sorption of Pb(II) ions onto the heterogeneous sites of the sorbent matrices, further justified by calculated intensity of adsorption ($0 \leq 1/n \leq 1$) and

the correlation coefficient values (R^2 nearer to unity), as suggested by K.S. Obayomi *et al.*,²³.

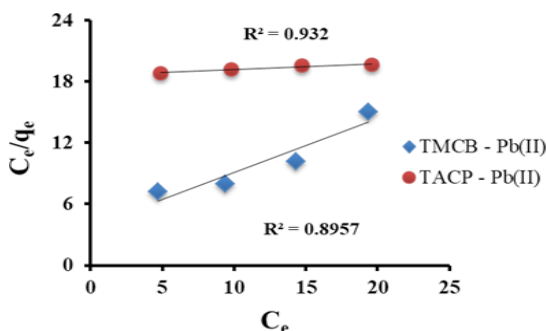


Fig. 16(a). Langmuir Isothermal Plot

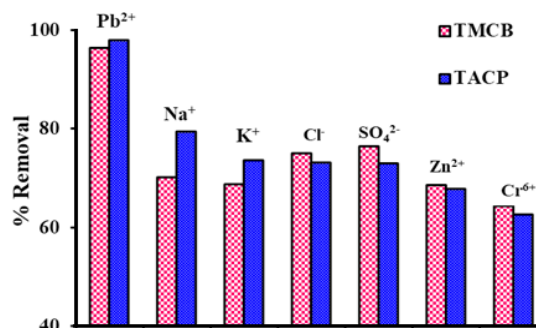


Fig. 15. Impact of Cations/Anions/Co-ions

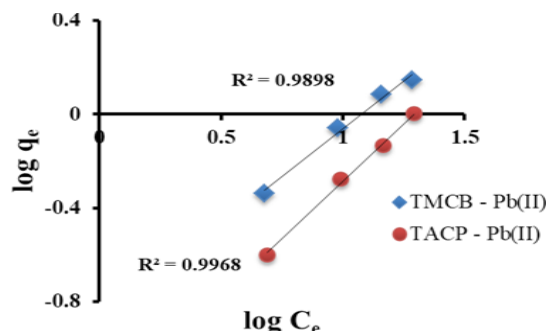


Fig. 16(b). Freundlich Isothermal Plot

Table 1: Isothermal Constants

System	q_m (mg/g)	Langmuir K_L (L/mg)	R^2	$1/n$	Freundlich K_f (L/mg)	R^2
TMCB – Pb(II)	1.89	7.19	0.8957	0.82	0.13	0.9898
TACP – Pb(II)	17.06	37.68	0.9320	0.98	0.05	0.9968

CONCLUSION

Magnolia champaca Bark and Attapulgitte clay powder were collected, modified using 0.1N HCl to maximize their surface area and utilized as an effective sorbents in the chelation of Pb(II) ions from the hydrous environment. The morphological features of the unloaded and loaded samples were analyzed using SEM and EDAX equipment. Peak variations pertaining to functional groups of the modified/ metal laden sorbents were assessed by FTIR spectral studies. Operating factors for the TMCB–Pb(II)/TACP–Pb(II) systems were optimized as 0.18 mm particle size; pH 5 and 20 mg/L initial concentration with a maximum removal of 96%/98%, with variations in agitation time intervals as 15 mins/9 mins at temperatures 313 K/303 K correspondingly. Metal trapping

efficiencies of the selected sorbents were hindered in the presence of co-metal ions justified by their corresponding ionic radii property. Linearity and better fit of the experimental data was found to be well in Freundlich isotherm model. Treated *Magnolia champaca* Bark and Attapulgitte clay powder exhibited excellent isolation property towards the noxious Pb(II) ions, thereby their efficacy shall be explored in the confiscation of other toxic metals.

ACKNOWLEDGMENT

Authors acknowledge the DST FIST, New Delhi, India for the infrastructure provided.

Conflict of Interest

The authors declare no conflict of interest.

REFERENCES

1. Ukaogo P. O.; Ewuzie U.; Onwuka C. V., *Microorganisms for Sustainable Environment and Health, Elsevier.*, **2020**, 419–429.
2. Tran H. N.; Chao., *Environ Sci Pollut Res.*, **2018**, 1–13.
3. Speight J. G.; *Natural Water Remediation Chemistry and Technology, Butterworth–Heinmann*, **2020**, 165–198.
4. Ledezma C. Z.; Bolagay D. N.; Figueroa F.; Ledezma E. Z.; Ni M.; Alexis F.; Guerrero V. H., *Environ. Technol. Innov.*, **2021**, 22, 1-26.
5. Sen A.; Pereira H.; Olivella M. A.; Villaescusa I., *Int. J. Environ. Sci. Technol.*, **2014**, 1–14.
6. Khokhar A.; Siddique Z.; Misbah., *J. Environ. Chem. Eng.*, **2015**, 1–9.
7. Raj K.; Das A. P., *Envtl. Chem. And Ecotox.*, **2023**, 5, 79–85.
8. Kumar A.; Pinto, M.M.S.C.; Chaturvedi A. K.; Shabnam A. A.; Subrahmanyam G.; Mondal R.; Gupta D. K.; Malyan S. K.; Kumar S. S.; Khan S. A. and Yadav K. K., *Int. J. Environ. Res. Public Health.*, **2020**, 17, 1-33.
9. Bashir A.; Malik L. A.; Ahad S.; Manzoor T.; Bhat M. A.; Dar G. N.; Pandith A. H., *Environ. Chem. Lett.*, **2018**, 17(2019), 729–754.
10. Chai W. S.; Cheun J. Y.; Kumar P. S.; Mubashir M.; Majeed Z.; Banat F.; Ho S.; Show P. L., *J. Clean. Prod.*, **2021**, 296, 1-16.
11. Anastopoulos I.; Pashalidis I.; Bandegharaei A. H.; Giannakoudakis D. A.; Robalds A.; Usman M.; Escudero L. B.; Zhou Y.; Colmenares J. C.; Delgado A. N.; Lima E. C., *J. Mol. Liq.*, **2019**, 295, 1- 17.
12. Saxena A.; Bhardwaj M.; Allen T.; Kumar S.; Sahney R., *Water Sci.*, **2017**, 1-9.
13. Quyen V.; Pham T. H.; Kim J.; Thanh D.; Thang P. Q.; Van Le Q.; Jung S. H.; Kim T. Y., *Chemosphere.*, **2021**, 284, 1–7.
14. Pathirana C.; Ziyath A. M.; Jinadasa K.B.S.N.; Egodawatta P.; Sarina S.; Goonetilleke A., *Chemosphere*, **2019**, 234, 488–495.
15. Wierzba S.; Kłos A., *J. Clean. Prod.*, **2019**, 225, 112–120.
16. Sadeeka S. A.; Negmb N. A.; Hefni H.H.; Abdel Waha M. M., *Int. J. Biol. Macromol.*, **2015**, 81, 400–409.
17. Geetha P.; Latha M.S.; Pillai S. S, Koshy M., *Ecotoxicol. Environ. Saf.*, **2015**, 122, 17–23.
18. Ashfaq A.; Nadeem R.; Bibi S.; Rashid U.; Hanif M. A.; Jahan N.; Ashfaq Z.; Ahmed Z.; Adil M. and Naz M., *Water.*, **2021**, 13, 1–15.
19. Rathi B. S.; Kumar P. S., *Environ. Polln.*, **2021**, 280, 1–19.
20. Ewis D.; Ba-Abbad, M. M.; Benamor A.; El-Naas M. H., *Appl. Clay. Sci.*, **2022**, 229, 1–31.
21. Akpomie K. G.; Dawodu F. A., *J. Adv. Res.*, **2015**, 6, 1003–1013.
22. Jingyan S.; Jing Y., *Adv. Mat. Res.*, **2012**, 446-449, 2960-2963.
23. Obayomia K.S.; Autab M.; Kovo A.S., *Desalin. Water. Treat.*, **2020**, 181, 376–384.